arXiv:cond-mat/9701045v1 [cond-mat.dis-nn] 8 Jan 1997

Univ.Roma I, 1146/96
cond-mat/9701045

A Study of Activated Processes in Soft Sphere Glass

David Lancaster[(a)] and G. Parisi[(b)]

[(a)]Van der Waals – Zeeman Lab.,
University of Amsterdam,
Valkenierstraat 65,
1018XE Amsterdam.

[(b)]Dipartimento di Fisica and INFN,
Università di Roma I *La Sapienza*,
Piazza A. Moro 2, 00185 Roma.

Abstract: On the basis of long simulations of a binary mixture of soft spheres just below the glass transition, we make an exploratory study of the activated processes that contribute to the dynamics. We concentrate on statistical measures of the size of the activated processes.

12/96

[(a)] (lancaste@phys.uva.nl)
[(b)] (parisi@roma1.infn.it)

1. INTRODUCTION AND MOTIVATION

It is well known that the relaxation times in glasses become extremely long when the glass transition is approached [1]. In fragile glasses, the relaxation times definitely increase faster than a simple Arrenius behavior, for example the viscosity can be fitted by the Volger-Fulcher law, $\exp(A/(T-T_0))$. In the standard picture of activated dynamics, this increase of the relaxation times implies an increase of the energy barriers relevant to relaxation processes. A divergence of the energy barriers at T_0 can hardly be explained without assuming some form of cooperative behaviour. Indeed, most theoretical proposals to explain fragile glass behaviour assume that the dynamics is dominated by very slow processes in which a large number of particles are rearranged [2].

Extensive numerical simulations have been performed on glasses [3][4], and the behaviour of the diffusion constant (whose definition involves just a single particle) has been carefully studied. Unfortunately there are practically no studies of the relaxation processes which occur in glasses and of their morphology (for example, the number of particles involved and their displacements). One of the most notable exceptions is the study of ref [5] where a rearrangement of 4 particles was observed.

The aim of the present study is essentially exploratory. We simulate a binary mixture of soft spheres just below the glass temperature and address ourselves to the problem of identifying the activated processes and of studying their properties in a systematic statistical way. We present the techniques we have used and the results we have obtained. We have concentrated most of our attention on the number of particles involved, or rather the spatial extent of the activated process, and we present two different techniques to compute this size. A careful study of the temperature dependence of the quantities that we have measured would be extremely interesting, but it goes beyond the limits of this work. Detailed theoretical predictions for these quantities would also be welcome and we hope that this note will stimulate research.

The paper is organized as follows: sections 2,3 and 4 describe the simulation data and the remaining sections 5,6 and 7 are concerned with the analysis of activated processes. In section 2 we discuss the model and the simulations that we have performed, section 3 deals with the issue of thermalisation and in section 4 we analyse our data using some of the distributions usually considered. In section 5 we consider the technique of cooling to accurately find jumps and count them, sections 6 and 7 deal with two methods of viewing the spatial distribution of the displacements associated with the activated processes. Because the study is exploratory, we give no conclusion.

2. THE SIMULATIONS

2.1. The Model

We use a Molecular Dynamics (MD) approach with leapfrog algorithm [6]. Because our goal is to look in detail at the activated processes underlying the dynamics, a small system is acceptable and we have used this to advantage in writing a simple yet fast code running on APE [7] by directly summing over all atom pairs rather than deal with the complications of neighbour lists that are not simple on multi-processor machines.

We consider a total of $N = 512$ spheres in a periodic box $8 \times 8 \times 8$, and use a standard technique to prevent the system crystalising by working with a 50% mixture of two different types of sphere with different effective radii [5]. The sphere species label is written $\alpha = 1, 2$, the radii are σ_α and the potential between spheres is,

$$V_{\alpha\beta} = \left(\frac{\sigma_{\alpha\beta}}{r}\right)^{12} \tag{2.1}$$

Where, $\sigma_{\alpha\beta} = (\sigma_\alpha + \sigma_\beta)/2$. In this work we choose $\sigma_1 = 1.0$ and $\sigma_2 = 1.2$. The masses of the spheres are both set equal to one.

This system of soft spheres and its variants have been studied extensively [3,5] and the value of the melting and glass transition are known. The melting transition occurs at $T = 1.76 \pm 0.06$ [8] while the glass transition is at $T = 0.56 \pm 0.01$ [3]. We shall work in the vicinity of $T = 0.5$, just below the glass transition where the dynamics is mainly due to the activated processes. This is in contrast to the situation at higher temperature where smoother mechanisms are responsible for diffusion. Indeed, the numerical method for finding the glass transition temperature is as the temperature at which the smooth processes give vanishing diffusion.

2.2. Data sets

We have collected four data sets starting with different initial configurations; let us call them A,B,C,D. The individual characteristics of each one, and the details of the initial state preparation are discussed in the appendix. Each data set is nominally at $T = 0.5$ and has the same molecular dynamics parameters: that is a time step of 0.002 and a sampling of the configuration every 10^4 such molecular dynamics steps (corresponding to a time interval of 20 units). The total run time for each data set is always greater than 10^5, but varies between data sets; A: 2.6×10^5, B: 5.2×10^5, C: 1.4×10^5, D: 1.8×10^5. A and B are the most interesting data sets, and for this reason, the longest. We find that the runs C and D are not really long enough to obtain good statistics, but we have retained them for the purpose of comparison.

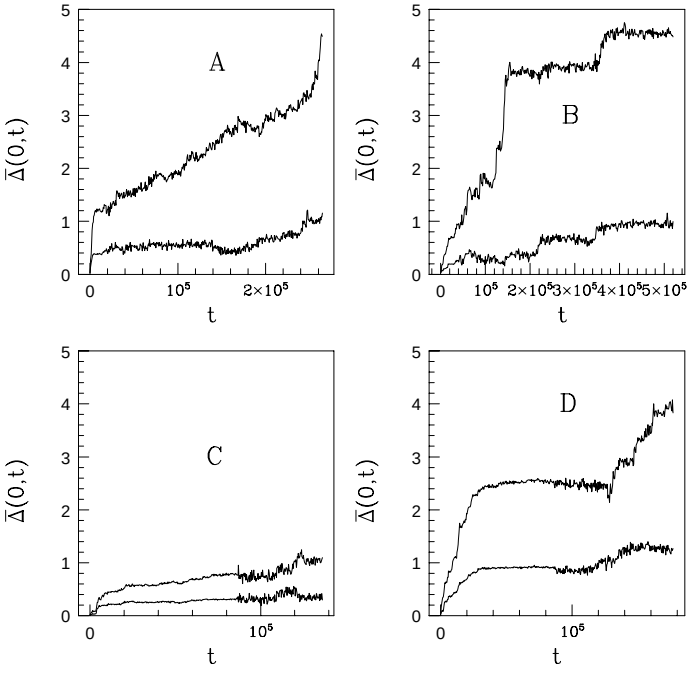


Fig. 1: Mean squared movement with respect to first configuration of the run, small spheres (upper lines), and large spheres (lower lines). Note that the time axis is scaled differently for the different length runs.

2.3. Displacement

The probability distribution for the distances moved by each sphere after a given time gives a good initial idea of the processes we are interested in analysing. The simplest quantity to consider is the mean squared distance moved. When this is calculated in a periodic geometry there is some latitude in the precise way of taking account of spheres that have migrated around the periodic borders. Here we have stored the configurations in such a way as to keep track of this information by writing the coordinates, $x \in (-\infty, \infty)$, as the periodic part, $x_{pbc} \in (0, L)$, plus the winding part that is an integral multiple of L. We define the movement $\Delta_i(t, t')$ of the i th sphere between times t and t' using coordinates with the centre of mass ($\overline{\mathbf{r}} = \frac{1}{N}\sum_i \mathbf{r}_i$) removed.

$$\Delta_i(t, t') = \left|\mathbf{r}_i(t) - \mathbf{r}_i(t')\right|^2 \tag{2.2}$$

The mean squared movement is then,

$$\overline{\Delta}(t, t') = \frac{1}{N}\sum_i \Delta_i(t, t') \tag{2.3}$$

In figure 1 we show the mean squared movement with respect to the first configuration. There are wide variations in behaviour because the small temperature differences between the data sets have a large effect on the rate of diffusion. Note that in this, and subsequent figures the time axis is scaled differently according to the length of the different data sets. This figure indicates that the movement is not smooth, but progresses by a series of jumps which correspond to the activated processes we are interested in.

3. THERMALISATION

Because we work at temperatures slightly below the glass transition, it is essential to discuss to what degree equilibrium is achieved and to what extent our simulations are representative.

The molecular dynamics is at constant energy without any rescaling of momenta for stability during the course of the simulations. Our choice of MD time step is conservatively small, and the total energy always remained stable throughout the runs to an accuracy of order 0.001. No consistent drift was apparent even over the very longest time scales in data set B.

The data sets A and D are at slightly higher total energy than the other pair and each run is at a slightly different temperature. The table below shows the values of the energies averaged over the duration of each complete run.

Data Set				
	A	B	C	D
Total E	7.326	7.261	7.254	7.330
Kinetic E	0.79	0.77	0.76	0.80
Potential E	6.54	6.49	6.50	6.53

Table 1: Average energies for each data set, after removal of a thermalisation period of 0.5×10^5 (see discussion at the end of this section).

Data sets C and D are at slightly low and high temperatures respectively and correspondingly we find few jumps in C and smoother behavior in D.

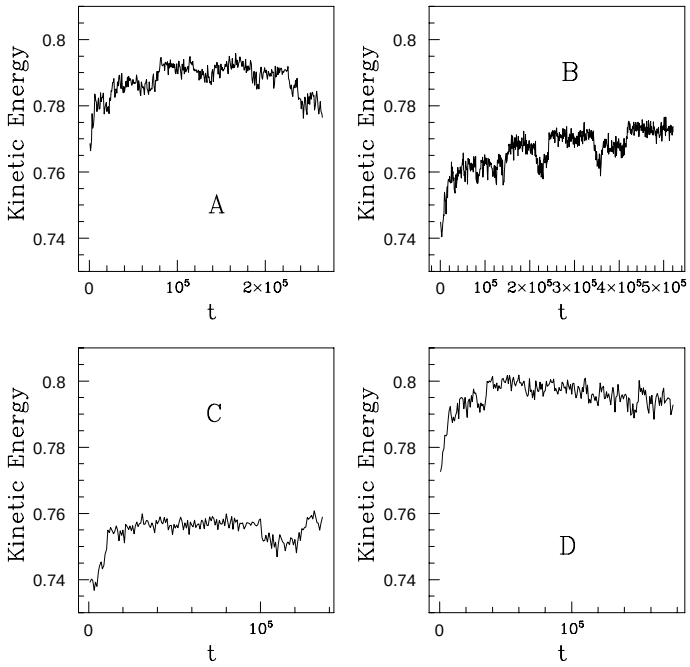


Fig. 2: Kinetic energy against time. Each point has been averaged over 200 measurements taken over a period of 800 time units (corresponding to 40 configurations).

We have not given errors in the table because there is some consistent relaxation during the course of the runs which becomes clear on a closer investigation of the kinetic energy shown in figure 2. The potential energy decreases slightly and the kinetic part increases. This is most noticeable in the beginning part of the plots where it indicates insufficient thermalisation in the preparation of the initial states. However, it is also clear that even over the very long time scales of data set B that relaxation continues.

These observations suggest that the system relaxes to a lower potential well in the energy surface. That this process can be seen in simulations is indicative of the smallness of the system and the very long runs. With these data it is not possible to deduce anything concerning dependence on the method of preparing the initial sample.

Another sign of the relaxation comes from the size of the move between subsequent configurations. Since this data is relevant to later developments we show it here. In fig. 3 the value of $\Delta(t, t+20)$ between successive configurations is plotted. Each data point is averaged over 100 configurations. Again an initial relaxation is apparent. It is noticeable that even over the very long run B, there are significant variations in the degree of activity.

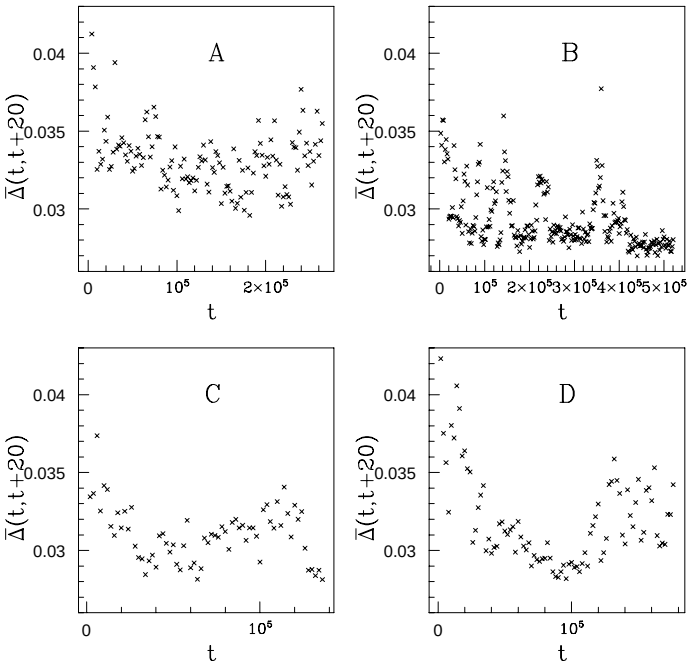


Fig. 3: Relaxation of average step movement with time. Each point has been averaged over 100 measurements taken over a period of 2000 time units.

In subsequent sections where we consider time averaged quantities we have removed an initial thermalisation period from the start of each data set. The length of this thermalisation period has been fixed at 0.5×10^5 time units from a study of fig. 2 and fig. 3. We see that this procedure still leaves some long time relaxation and variation in degree of activity in the case of B. This observation throws some light on the puzzling behaviour of the lowest temperature data set, C, which shows a suprisingly high degree of activity in fig. 3 despite its small overall movement shown in fig. 1. It seems likely that the whole of the run C corresponds to one of the active periods of B and that a thermalisation time longer than 0.5×10^5, and in fact longer than the whole run, is needed. This should be bourne in mind for later analyses.

4. DIFFUSION DISTRIBUTIONS

Various probability distributions of the step movement have been investigated at higher temperatures in the work of Hansen *et al.* [3] for soft spheres and more recently for

Leonard Jones spheres by Kob and Andersen [4]. We first consider the probability distribution of the movements of the individual spheres between configurations, $P_1\big(\Delta(t, t+20)\big)$. This is defined as,

$$P_1(\Delta) = \frac{1}{N} \sum_i \delta\big(\Delta - \Delta_i(t, t+20)\big) \tag{4.1}$$

When calculated for a single pair of configurations, the distribution is noisy but the tail corresponding to activated processes is visible in cases where there is a jump.

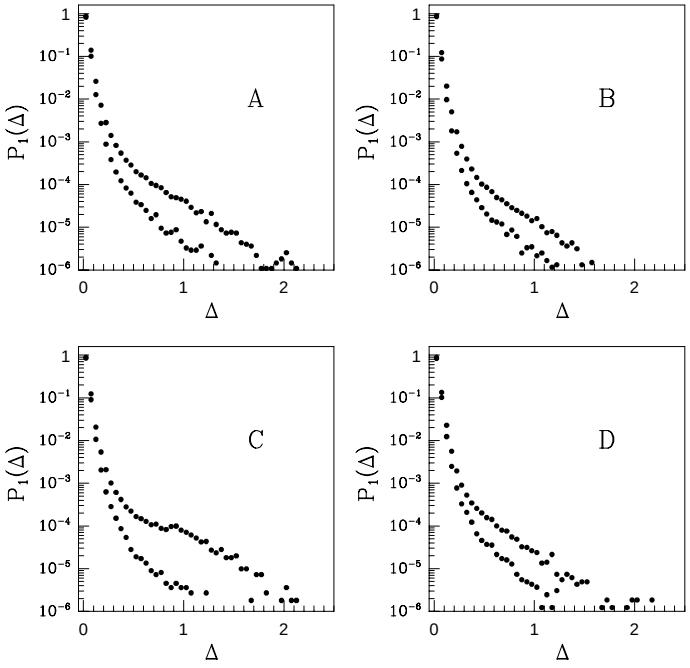


Fig. 4: Averaged probability distribution of step movement, $P_1(\Delta)$, shown with a logarithmic scale. Upper and lower curves are for small and large spheres respectively.

In figure 4 we show this quantity averaged over the time duration of the data set (with initial thermalisation period removed). We use a logarithmic scale to see the small contribution of large motions.

The tail of the distribution shows behavior indicative of diffusion since the probability distribution decays exponentially with Δ. The diffusion is due to the activated processes, in contrast to the situation at higher temperature where smoother mechanisms are responsible. The time step of 20 units is not long enough to justify the distribution one would expect from diffusion, $\sim \exp(-\Delta/4Dt)$. If nevertheless we use this formula to define an

effective diffusion constant, we find values of order, $3 \sim 4 \times 10^{-3}$, which are somewhat larger than the values found by other methods in [3].

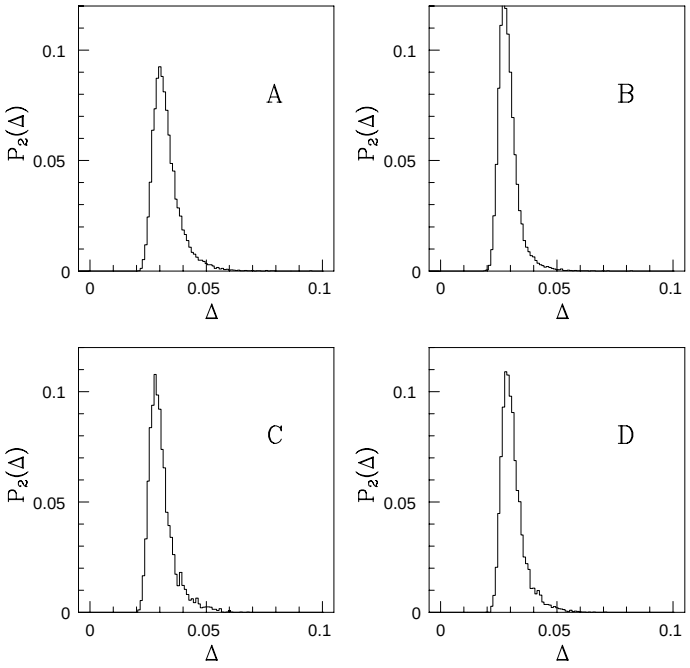


Fig. 5: Probability distribution of mean squared step movement, $P_2(\Delta)$. Shown only for small spheres.

It is sometimes useful to consider probability distributions in time. In fig. 5 we show the probability distribution of the mean square step displacement, $P_2(\overline{\Delta}(t, t+20))$. For a run of S configurations this is defined as,

$$P_2(\Delta) = \frac{1}{S} \sum_{t}^{S} \delta\big(\Delta - \overline{\Delta}(t, t+20)\big) \tag{4.2}$$

In comparison with (4.1), this probability distribution shows the variations in time of a spatially averaged movement. The tail should indicate the likelihood of jumps, but there is not sufficient data to determine its behavior accurately. One would expect a tall narrow peak with small tail at low temperature, and a somewhat wider peak shifted to larger $\overline{\Delta}$ at higher temperature. Comparison of A and B correctly identifies their temperature ordering, but there is insufficient data to make similar statements with regard to the shorter runs C and D.

5. COOLING AND LOCATING JUMPS

5.1. Cooling

We have already seen that the motion of the system does not proceed smoothly, but rather by a series of jumps. We now turn our attention to a detailed analysis of these activated processes. The most clear definition of an activated process would be a movement between different potential wells. This can only be determined unambiguously in the absence of thermal fluctuations and motivates us to study configurations that have been cooled to zero temperature.

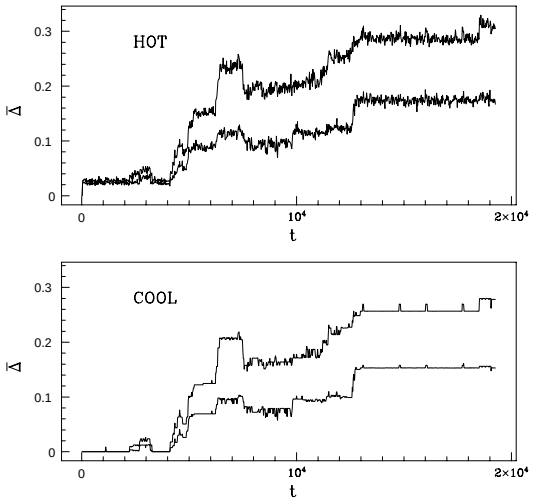


Fig. 6: Comparison of hot and cooled data for a fairly active period of 0.2×10^5 time units taken from data set B. Mean squared displacement, $\overline{\Delta}$, is shown with respect to the first configuration of this time interval.

The method of cooling we chose was to introduce an effective friction into the MD equations by reducing the momenta by a factor of 0.998 each time step. This technique was found to be more efficient than a steepest descent type method in which the initial momenta are ignored. We made 5000 MD steps to cool each configuration and typically reduced the kinetic energy to order 10^{-5}. We have not cooled all configurations obtained, but have decided to look at a fairly active part of the time evolution of data set B consisting of a period of 0.2×10^5 time units fairly early in the complete run. We have cooled the 1000 configurations from 3854 to 4854 of data set B. The effect of cooling is clearest if we consider the total movement in the cooled set and compare with the original hot data. Inspection of fig. 6 makes it clear how thermal noise is removed.

In this time period we find 261 jumps which can be classified as one of two types. Some of the jumps merely interchange a small number of particles and simply amount to a relabeling of the configuration, whereas others are less simple and change the energy. For example, in the first class we have seen motions which only relabel between 2 and 5 particles, with all other particles remaining fixed. In the other class the major part of the movement is still local, but all other particles must move by a small amount in order to accommodate the new configuration. In this case it is less easy to say how many particles are involved in the jump. The potential energy change occurring in the second class of jump is sometimes very small and only related to a metastable state. In these circumstances the cooling is providing excessive information about small features of the potential surface which would be washed out in a finite temperature simulation. This effect is also apparent in the cool plot of fig. 6 where many of the 261 jumps are small and should not be regarded as important processes.

	COOL	HOT
All jumps	0.271	$\sim$
$\overline{\Delta} > 0.01$	0.089	1.0
$\overline{\Delta} > 0.02$	0.017	1.0
$\overline{\Delta} > 0.03$	0.002	0.411
$\overline{\Delta} > 0.04$	0.0	0.074
$\overline{\Delta^2} > 0.002$	0.133	0.368
$\overline{\Delta^2} > 0.003$	0.091	0.201
$\overline{\Delta^2} > 0.004$	0.069	0.154
$\overline{\Delta^2} > 0.005$	0.060	0.117
$\Delta_{max} > 0.3$	0.184	0.300
$\Delta_{max} > 0.4$	0.156	0.209
$\Delta_{max} > 0.5$	0.128	0.163
$\Delta_{max} > 0.6$	0.086	0.128

Table 2: Fraction of jumps with size (according to various criteria) greater than some cutoff. Shown for the set of 1000 cooled configurations and their hot counterparts.

Given this technique of unambiguously finding jumps in the cooled data it is interesting to see whether their presence can be accurately predicted by a study of the hot data. A direct procedure would be to introduce a cutoff on the displacement. We find that this

certainly captures the larger jumps in the cooled data, but not all the smaller ones. On the other hand, as mentioned above, small moves found by the method of cooling need not have any significance. A good cutoff is a matter of empirical choice; in table 2 we consider cutoffs in the mean squared displacement $\overline{\Delta}(t, t+20)$, the mean quartic displacement $\overline{\Delta^2}(t, t+20)$ and the maximum (amongst the spheres) step size $\Delta_{max}(t, t+20)$. A cutoff on the energy change is not effective. We use the same cutoff for large and small species of sphere, but in effect it is always the small spheres that signal a jump. We show the fraction of jumps found in this cooled set of configurations calculated using each criterion. The thermal motion makes a cutoff in $\overline{\Delta}$ insensitive and we shall discard this method. Of the other choices, the cutoff on Δ_{max} seems to give closer results between the hot and cool data so we prefer this technique.

	Data Set			
	A	B	C	D
$\Delta_{max} > 0.3$	0.374	0.192	0.407	0.264
$\Delta_{max} > 0.4$	0.235	0.105	0.212	0.171
$\Delta_{max} > 0.5$	0.165	0.071	0.146	0.122
$\Delta_{max} > 0.6$	0.119	0.050	0.113	0.084

Table 3: Fraction of jumps with size (Δ_{max}) greater than some cutoff. Shown for complete thermalised data sets.

Having identified suitable ranges for the cutoffs we use the same method to analyse the complete thermalised data sets. Table 3 shows the fraction of jumps observed throughout the runs.

From a comparison of the tables it is clear that the set of configurations we cooled were indeed more active than the average of data set B. In table 3, A has a larger fraction of jumps than B, as we would expect since it is slightly warmer. The shorter runs, C and D, do not however fit this pattern, presumably because of their limited data.

In a later section we will use this method to identify jumps and will fix the cutoff at the conservative end of the range, $\Delta_{max} > 0.6$, in order to eliminate spurious processes relating to metastable states.

5.2. Viewing Activated Processes

Activated processes are local disturbances and an intuitive way of visualising them is to locate the centre and plot the radial variation in the move size.

We choose to define the centre as the mean position weighted by the displacement.

$$\mathbf{r}_c = \frac{\sum_i \mathbf{r}(\Delta_i)^\alpha}{\sum_i (\Delta_i)^\alpha} \tag{5.1}$$

It does not correspond to the location of any particle. Because of the periodic boundary conditions this definition actually requires some prior guess which is obtained from the location of the largest move. For cooled data the method is then straightforward, but for hot data another complication arises. Random thermal movements of spheres distant from the true centre contribute excessively to the mean and must be suppressed. We do this by weighting with a power, α, of the movement, rather than the movement itself. Empirically, a power of $\alpha = 2$ (corresponding to weights Δ^2) is found to be adequate.

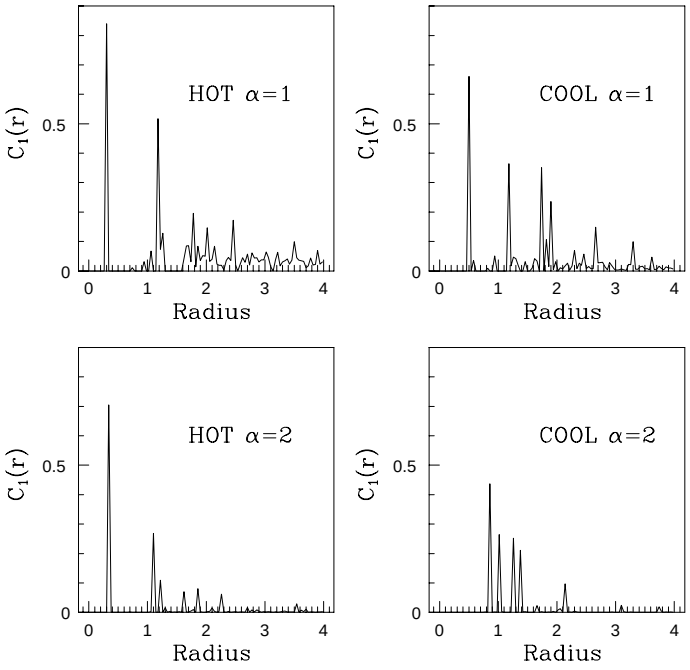


Fig. 7: Example of the movement of spheres plotted against the distance from the centre of the jump. Hot (left) and cooled (right) data, and different weight factors Δ (top) and Δ^2 (bottom). The example comes from configuration 4075 to the subsequent configuration of data set B. The location of the centre varies slightly in each plot.

Once the centre is defined, the radial distribution is given by,

$$C_1(r) = \frac{\sum_i \Delta_i^\alpha \delta\big(r - |\mathbf{r}_i - \mathbf{r}_c|\big)}{\sum_i \delta\big(r - |\mathbf{r}_i - \mathbf{r}_c|\big)} \tag{5.2}$$

Figure 7 shows an example of this distribution for a particular jump involving quite a large number of particles. The plot is repeated with both hot and cooled data and also using Δ and Δ^2 in the weighting factor. The effectiveness of the weighting factor in reducing thermal noise at large radius is apparent.

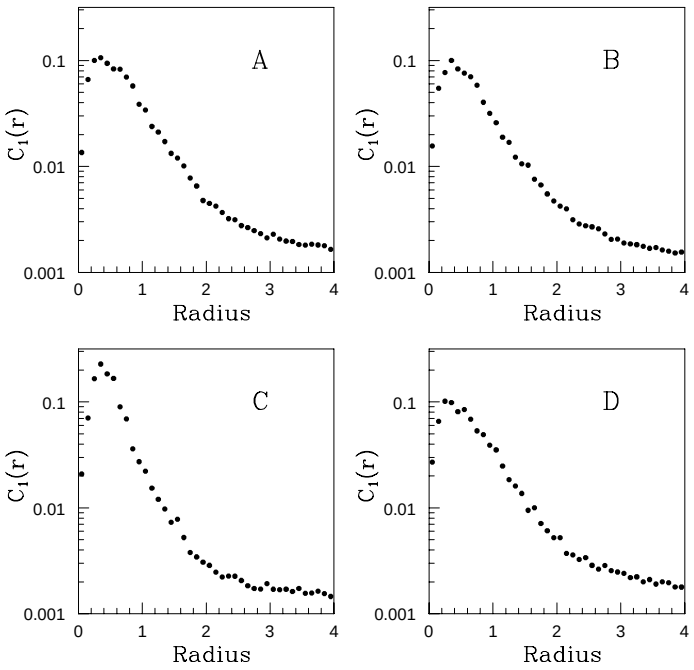


Fig. 8: Averaged movement of spheres, $C_1(r)$, plotted against the distance from the centre of the jump. Using hot data with a cutoff, $\Delta_{max} > 0.6$ on all thermalised data. We have used the weighting power $\alpha = 2$.

In applying the method to hot data it is important that a jump is truly present, otherwise the centre will correspond to the location of some slightly larger than average random movement. To check that there is a jump, a cutoff on the maximum move can be introduced as discussed in the previous section. In figure 8 we use this technique to show an averaged form of the distribution $C_1(r)$. We impose the conservative requirement for a jump by taking the average only over jumps characterised by $\Delta_{max} > 0.6$ in the thermalised data. We have plotted the distribution using a logarithmic scale to bring out

the small contributions at large radius from the centre. The variation between runs of the mean size for the jumps is too small to be able to analyse temperature dependence.

In summary; this technique is helpful for intuition in seeing individual jumps but relies on too many parameters to be a good statistical measure for activated processes.

6. CORRELATION

In this section we present an alternative method of determining the size of movement without the need to prejudge the presence of a jump by introducing a cutoff. We evaluate correlations between the displacements of different spheres by calculating the following,

$$C_2(r) = \frac{\sum_{ij,|\mathbf{r}_i-\mathbf{r}_j|<R} \left(\Delta_i(t,t+20) - \overline{\Delta}\right)\left(\Delta_j(t,t+20) - \overline{\Delta}\right)\delta(r-|\mathbf{r}_i-\mathbf{r}_j|)}{\sum_{ij,|\mathbf{r}_i-\mathbf{r}_j|<R}\delta(r-|\mathbf{r}_i-\mathbf{r}_j|)} \qquad (6.1)$$

The quantity in the denominator is well known as the structure function. In the numerator, note that we have subtracted the mean value of the displacement. This avoids the difficulties experienced in the previous method of requiring weighting by powers of Δ in order to suppress long distance thermal motion. R is the maximum distance on the periodic volume, which is 4.0 in our case.

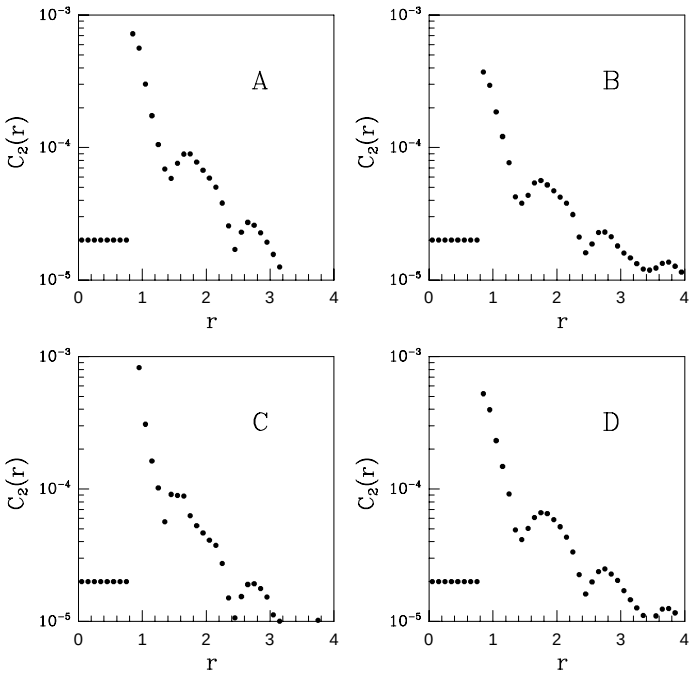


Fig. 9: Correlations, $C_2(r)$, averaged over thermalised data. An offset of 2×10^{-5} has been added to allow a logarithmic axis.

The quantity $C_2(r)$ contains little information when evaluated at a single time for a pair of configurations. But when averaged over the runs as shown in fig. 9 it displays interesting structure. We see some oscillation as we expect for a quantity similar to the structure function, but the major contribution is from adjacent spheres. Since $C_2(r)$ tends to go slightly negative at large r we have added a constant offset in order to be able to use a log scale. This offset is clear in the figure since it corresponds to the plateau at small r where $C_2(r)$ strictly vanishes. The mean jump size, $\int C(r)rdr$, varies little between runs.

It would be interesting to have theoretical predictions and better measurements for the temperature dependence of this correlator.

Acknowledgements

DL would like to thank the British Council and the Consiglio Nazionale delle Ricerche for financial support during part of this work.

Appendix . Initial States of A,B,C,D.

In this appendix we discuss the individual characteristics of the data sets A,B,C,D, and the details of the initial state preparation.

All the initial configurations derive from a high temperature molecular dynamics run sampled at time intervals that yield independent configurations. To be precise, the high temperature is $T = 8.0$ where we use a version of molecular dynamics that renews momenta from a gaussian distribution every 5000 steps with time step 0.001. The initial thermalisation is of 3 million steps (corresponding to a total movement per particle of $\overline{\Delta} \sim 2 \times 10^4$), then four configurations are taken at intervals of 5×10^5 steps (which corresponds to a movement per particle of $\overline{\Delta} \sim 3.6 \times 10^3$). These four independent configurations are then treated as follows.

A) An slow annealing of 3 million steps down to $T = 0.5$. The last configuration of the annealing is the initial configuration for data set A.

B) A more abrupt annealing of 7.5×10^5 steps down to $T = 0.5$ followed by a pre-thermalisation consisting of 4×10^5 steps with momentum updates intended to stabilise the temperature. It is some of the later configurations of this data set, B, that have been cooled as discussed in section 5.

C) A direct quench down to $T = 0.5$ by rescaling the momenta followed by a brief pre-thermalisation consisting of 2000 steps. No jumps of the type in figure 1 are observed in this data set which is at a slightly lower temperature, and it has therefore not been extended as far as A or B.

D) A history like that of set B, with an annealing followed by pre-thermalisation with the same parameters as B. In this case the temperature turns out to be slightly higher than in the other runs and for this reason the jumps we observe are not very sharp.

References

[1] For reviews see, W. Gotze, *Liquid, freezing and the Glass transition*, Les Houches (1989), J.P. Hansen, D. Levesque, J. Zinn-Justin editors, North Holland;
C.A. Angell, Science, **267**, 1924 (1995).

[2] G. Adams and E.A. Gibbs, J.Chem.Phys. **43**, 139 (1965).

[3] B. Bernu, Y. Hiwatari and J.P. Hansen, J.Phys. **C18**, L371 (1985);
B. Bernu, J.P. Hansen, Y. Hiwatari and G. Pastore, Phys.Rev. **A36**, 4891 (1987);
J.N.Roux, J.L. Barrat and J.P. Hansen, J.Phys. **C1**, 7171 (1989).

[4] W. Kob and H.C. Andersen, Phys.Rev. **E51**, 4626 (1995);
Phys.Rev. **E52**, 4134 (1995).

[5] H. Miyagawa, Y. Hiwatari, B. Bernu and J.P. Hansen, J.Chem.Phys **88**, 3879 (1988).

[6] D.C. Rapaport, *The Art of Molecular Dynamics Simulation*, C.U.P. (1995).

[7] See for example, C. Battista *et al*, Int.J.High Speed Comput. **5**, 637 (1993);
the use of APE for molecular dynamics simulations is also discussed by L.M. Barone, R. Simonazzi and A. Tenenbaum, Roma I preprint.

[8] J.P. Hansen, Phys.Rev. **A2**, 221 (1970);
W.G. Hoover, M. Ross, K.W. Johnson, D. Henderson, J.A. Barker and B.C. Brown, J.Chem.Phys. **52**, 4931 (1970).